

Prying Apart Ruddlesden–Popper Phases: Exfoliation into Sheets and Nanotubes for Assembly of Perovskite Thin Films

Raymond E. Schaak and Thomas E. Mallouk*

Department of Chemistry, The Pennsylvania State University,
University Park, Pennsylvania 16802

Received June 19, 2000. Revised Manuscript Received September 5, 2000

Protonated Ruddlesden–Popper tantalates and titanotantalates $H_2[A_{n-1}B_nO_{3n+1}]$ ($A = Na, Ca, Sr, La; B = Ta, Ti$) that have acidic interlayer protons were exfoliated using tetra(*n*-butyl)ammonium hydroxide (TBA^+OH^-). $H_2CaNaTa_3O_{10}$ forms both single sheets and tubular “scrolls” when reacted to make $TBA_xH_{2-x}CaNaTa_3O_{10}$ colloids. In contrast, $TBA_xH_{2-x}A_2Ta_2TiO_{10}$ and $TBA_xH_{2-x}AlTa_2TaO_{10}$ ($A = Ca, Sr$) form sheets exclusively. The $n = 2$ tantalate $TBA_xH_{2-x}SrTa_2O_7$ forms high aspect ratio scrolls, as well as smaller amounts of sheets. In contrast to the analogous tantalates, the Ruddlesden–Popper titanates and titanoniobates have weakly acidic interlayer protons and exfoliate only to a limited extent. $TBA_xH_{2-x}SrNb_2O_7$ forms sheets exclusively, whereas $TBA_xH_{2-x}Ca_2Nb_2TiO_{10}$ forms both sheets and scrolls. The $n = 3$ titanate $H_2La_2Ti_3O_{10}$ exfoliates into sheets using *n*-butylamine, and $Na_2La_2Ti_3O_{10} \cdot xH_2O$ forms sheets when exfoliated with TBA^+OH^- . When reacted with *O*-(2-aminopropyl)-*O'*-(2-methoxyethyl) polypropylene glycol 500, $H_2La_2Ti_3O_{10}$ exfoliates into monodisperse 20×100 nm scrolls. The exfoliated tantalates and titanotantalates can be electrostatically adsorbed to a Si/SiO₂/PDDA [PDDA = poly(diallyldimethylammonium chloride)] surface, forming perovskite monolayers. Above pH 9.5, $TBA_xH_{2-x}SrLaTi_2TaO_{10}$ sheets tile to densely cover a Si/SiO₂ surface derivatized with 4-aminobutyldimethylmethoxysilane (4-ABDMMS) and two bilayers of poly(sodium styrenesulfonate) (PSS) and poly(allylamine hydrochloride) (PAH). The exfoliated titanates and titanoniobates generally do not adhere to polycationic surfaces.

Introduction

Perovskite-type transition-metal oxides¹ possess a wide variety of important properties, such as superconductivity,² colossal magnetoresistance,³ ferroelectricity,⁴ and catalytic activity,⁵ depending on the choice and stoichiometry of the A- and B-site cations. A number of the technological applications of perovskite-based materials rely on the ability to make particles, thin films, and ceramic bodies with controlled composition, crystal-

linity, and texture. Although much of the research in this area has focused on hydrothermal particle synthesis and vapor-phase film growth techniques, “soft” chemical techniques such as intercalation, exfoliation, and reassembly of lamellar precursors offer an interesting alternative.

In the past few years, advances in the electrostatic layer-by-layer self-assembly of thin film intercalation compounds have yielded high-quality multilayer films of clays,⁶ nanoparticles and platelets,⁷ and lamellar solid acids such as α -Zr(HPO₄)₂·H₂O⁸ and HTiNbO₅.⁹ Thin film heterostructures that have interesting electronic and photocatalytic properties have also been prepared.¹⁰ In all of these examples, colloidal particles derived from exfoliated lamellar solids are alternately stacked with

(1) Galasso, F. S. *Structure, Properties and Preparation of Perovskite-type Compounds*, Pergamon Press: Oxford, 1969.

(2) (a) Otszchi, K. D.; Poeppelmeier, K. R.; Salvador, P. A.; Mason, T. O.; Zhang, H.; Marks, L. D. *J. Am. Chem. Soc.* **1996**, *118*, 8951. (b) Salvador, P. A.; Greenwood, K. B.; Mawdsley, J. R.; Poeppelmeier, K. R.; Mason, T. O. *Chem. Mater.* **1999**, *11*, 1760.

(3) Moritomo, Y.; Asamitsu, A.; Kuwahara, H.; Tokura, Y. *Nature* **1996**, *380*, 141.

(4) (a) Brahmaraout, B.; Messing, G. L.; Trolrier-McKinstry, S.; Selvaraj, U. *Proceedings of the 10th IEEE International Symposium on Applications of Ferroelectrics*, Kulwicki, B. M.; Amin, A.; Safari, A., Eds.; IEEE: Piscataway, NJ, 1996; Vol II, pp 883–886. (b) Seabaugh, M.; Hong, S.-H.; Messing, G. L. In *Ceramic Microstructure: Control at the Atomic Level*; Tomsia, A. P.; Glaeser, A., Eds.; Plenum Press: New York, 1998; pp 303–310. (c) Takeuchi, T.; Tani, T.; Satoh, T. *Solid State Ionics* **1998**, *108*, 67. (d) Tani, T. *J. Korean Phys. Soc.* **1998**, *32*, S1217. (e) Horn, J.; Zhang, S. C.; Selvaraj, U.; Messing, G. L.; Trolrier-McKinstry, S. *J. Am. Ceram. Soc.* **1999**, *82*, 921. (f) Rehrig, P. W.; Park, S.-E.; Trolrier-McKinstry, S.; Messing, G. L.; Jones, B.; Shrout, T. R. *J. Appl. Phys.* **1999**, *86*, 1657.

(5) (a) Takata, T.; Furumi, Y.; Shinohara, K.; Tanaka, A.; Hara, M.; Kondo, J. N.; Domen, K. *Chem. Mater.* **1997**, *9*, 1063. (b) Kim, H. G.; Hwang, D. W.; Kim, J.; Kim, Y. G.; Lee, J. S. *Chem. Commun.* **1999**, 1077.

(6) Kleinfeld, E. R.; Ferguson, G. S. *Science* **1994**, *265*, 370.

(7) (a) Iler, R. K. *J. Colloid Interface Sci.* **1966**, *21*, 569. (b) Fendler, J. H.; Meldrum, F. *Adv. Mater.* **1995**, *7*, 607.

(8) (a) Kaschak, D. M.; Johnson, S. A.; Hooks, D. E.; Kim, H.; Ward, M. D.; Mallouk, T. E. *J. Am. Chem. Soc.* **1998**, *120*, 10887. (b) Kerimo, J.; Adams, D. M.; Barbara, P. F.; Kaschak, D. M.; Mallouk, T. E. *J. Phys. Chem. B* **1998**, *102*, 9451. (c) Kim, H.; Keller, S. W.; Mallouk, T. E.; Schmitt, J.; Decher, G. *Chem. Mater.* **1997**, *9*, 1414.

(9) Fang, M.; Kim, H. N.; Saupe, G. B.; Miwa, T.; Fujishima, A.; Mallouk, T. E. *Chem. Mater.* **1999**, *11*, 1526.

(10) (a) Kaschak, D. M.; Lean, J. T.; Waraksa, C. C.; Saupe, G. B.; Usami, H.; Mallouk, T. E. *J. Am. Chem. Soc.* **1999**, *121*, 3435. (b) Cassagneau, T.; Mallouk, T. E.; Fendler, J. H. *J. Am. Chem. Soc.* **1998**, *120*, 7848. (c) Feldheim, D. L.; Grabar, K. C.; Natan, M. J.; Mallouk, T. E. *J. Am. Chem. Soc.* **1996**, *118*, 7640. (d) Kaschak, D. M.; Mallouk, T. E. *J. Am. Chem. Soc.* **1996**, *118*, 4222.

polycationic layers to produce high-quality thin films that can be easily controlled at the nanometer level.¹¹

One of the requirements for using layer-by-layer assembly to prepare perovskite thin films with interesting physical properties is the availability of a wide variety of colloidal perovskite building blocks. A decade ago, Treacy et al. reported that the layered perovskite $\text{HCa}_2\text{Nb}_3\text{O}_{10}$ could be made to form unilamellar colloidal sheets by swelling the interlayer gallery to the point of delamination with a weak, bulky base.¹² Since then, these and related phases have been shown to adsorb to polycation-derivatized surfaces,¹³ and high-quality tiled monolayers and multilayer perovskite heterostructures can be self-assembled from these sheets.¹⁴

$\text{KCa}_2\text{Nb}_3\text{O}_{10}$, the alkali parent of $\text{HCa}_2\text{Nb}_3\text{O}_{10}$, belongs to the Dion–Jacobson family of layered perovskites,¹⁵ $A[A_{n-1}'B_nO_{3n+1}]$ (A = alkali, A' = alkaline earth or rare earth, B = transition metal). The protonated forms of most Dion–Jacobson phases are weak acids that readily intercalate organic bases with low to moderate $\text{p}K_b$ values.^{16–19} Protonated members of the Ruddlesden–Popper family of layered perovskites,²⁰ $A_2[A_{n-1}'B_nO_{3n+1}]$, are particularly interesting because they undergo topochemical dehydration to form three-dimensional perovskites. For example, HLaTiO_4 , an $n = 1$ Ruddlesden–Popper compound, dehydrates to $\text{La}_2\text{Ti}_2\text{O}_7$, which upon further heating transforms to a high T_c ferroelectric.²¹ A similar condensation reaction occurs with $\text{H}_2\text{SrM}_2\text{O}_7$ ($M = \text{Nb}, \text{Ta}$).²² Unfortunately, the protonated Ruddlesden–Popper compounds are difficult to manipulate as precursors to thin films and more complex structures, because in general they are known *not* to intercalate organic bases.¹⁸ Without the ability to intercalate bases, Ruddlesden–Popper phases are not useful as nanoscale building blocks. Gopalakrishnan and co-workers concluded from their study of $\text{H}_2\text{La}_2\text{Ti}_3\text{O}_{10}$ and $\text{H}_2\text{Ca}_2\text{Nb}_2\text{TiO}_{10}$ that the inability to intercalate organic bases is structural in nature, resulting from the staggered perovskite layers rather than the intrinsic acidity of the interlayer protons.¹⁸ On the other hand, Geselbracht and co-workers have shown recently that proton-exchanged Dion–Jacobson tantalates are more acidic than the analogous titanates and niobates.²³ This suggests that the Ruddlesden–Popper tantalates

should be more reactive with bases than their titanate or niobate counterparts.

Recently, we reported the synthesis of the new $n = 3$ Ruddlesden–Popper tantalates, $\text{K}_2\text{CaNaTa}_3\text{O}_{10}$, $\text{K}_2\text{Ca}_2\text{Ta}_2\text{TiO}_{10} \cdot 0.8\text{H}_2\text{O}$, and $\text{K}_2\text{SrLaTi}_2\text{TaO}_{10} \cdot 2\text{H}_2\text{O}$,²⁴ as well as the $n = 2$ phase $\text{K}_2\text{SrTa}_2\text{O}_7$.²² Interestingly, we find that the protonated forms of these compounds, which have staggered perovskite layers as in $\text{H}_2\text{La}_2\text{Ti}_3\text{O}_{10}$, intercalate the bulky tetra(*n*-butyl)ammonium (TBA^+) cation by reaction with the strong base TBA^+OH^- . Past a critical loading level,^{8d} TBA^+ ions swell the interlayer gallery to the point of delamination. Some of these compounds are suspended as unilamellar sheets, but others curl to form nanoscale tubular “scrolls”. In this paper, we present studies on the interlayer acidity of the Ruddlesden–Popper family of layered perovskites, as well as the first examples of exfoliated Ruddlesden–Popper phases. We further show that the exfoliated sheets and nanotubes can also be used as building blocks for assembling perovskite thin films.

Experimental Section

Synthesis, Ion-Exchange, and Exfoliation. Specific synthetic procedures have been described in detail elsewhere.^{18,24–26} $\text{K}_2\text{La}_2\text{Ti}_3\text{O}_{10}$, $\text{K}_2\text{SrTa}_2\text{O}_7$, and $\text{K}_2\text{Ca}_2\text{Nb}_2\text{TiO}_{10}$ were prepared by reacting stoichiometric amounts of intimately mixed K_2CO_3 , La_2O_3 , CaCO_3 , TiO_2 , and Nb_2O_5 at 1100 °C for 1 day. NaLaTiO_4 was prepared by firing a pellet of Na_2CO_3 , La_2O_3 , and TiO_2 at 950 °C for 30 min. $\text{K}_2\text{CaNaTa}_3\text{O}_{10}$ was prepared by heating stoichiometric amounts of KOH , CaCO_3 , Na_2CO_3 , and Ta_2O_5 to 1050 °C for 12 h, followed by 6 h at 1100 °C after an intermittent grinding. $\text{K}_2\text{Ca}_2\text{Ta}_2\text{TiO}_{10}$ was prepared from the direct reaction of KOH , CaCO_3 , Ta_2O_5 , and TiO_2 at 1300 °C for 60 min. $\text{K}_2\text{SrLaTi}_2\text{TaO}_{10}$ was prepared by reacting stoichiometric amounts of K_2CO_3 , SrCO_3 , La_2O_3 , TiO_2 , and Ta_2O_5 at 1300 °C for 12 h. $\text{K}_2\text{Sr}_2\text{Ta}_2\text{TiO}_{10}$ was prepared by heating stoichiometric amounts of K_2CO_3 , SrCO_3 , Ta_2O_5 , and TiO_2 at 1200 °C for 12 h. $\text{Li}_2\text{SrNb}_2\text{O}_7$ was prepared by firing stoichiometric amounts of Li_2CO_3 , SrCO_3 , and Nb_2O_5 at 1100 °C for 3 days with two intermittent grindings. In all cases, a 40% excess of the alkali source was used to compensate for loss due to volatilization.

$\text{H}_2\text{La}_2\text{Ti}_3\text{O}_{10}$, $\text{H}_2\text{Ca}_2\text{Nb}_2\text{TiO}_{10}$, $\text{H}_2\text{CaNaTa}_3\text{O}_{10}$, $\text{H}_2\text{Ca}_2\text{Ta}_2\text{TiO}_{10}$, $\text{H}_2\text{SrLaTi}_2\text{TaO}_{10}$, $\text{H}_2\text{Sr}_2\text{Ta}_2\text{TiO}_{10}$, and $\text{H}_2\text{SrNb}_2\text{O}_7$ were prepared by ion-exchanging the corresponding alkali compound in 1 M HNO_3 for 5 days at room temperature. $\text{H}_2\text{SrTa}_2\text{O}_7$ and HLaTiO_4 were prepared in a similar manner, using 0.1 M HNO_3 . In all cases, the acid was replaced daily to ensure complete exchange.

Exfoliation was typically achieved by reacting 0.5 g of the protonated solid with a 30-fold molar excess of tetra(*n*-butyl)ammonium hydroxide (TBA^+OH^-) in 100 mL of water at room temperature for 2–4 weeks. In some cases, other bases such as *n*-butylamine and *O*-(2-aminopropyl)-*O'*-(2-methoxyethyl) polypropylene glycol 500 (Aldrich) were used.

Electrostatic Assembly of Perovskite Thin Films. Colloidal suspensions of sheets and scrolls were prepared by allowing the concentrated exfoliated suspensions to settle for a few hours (or overnight) and then removing the liquid near the top of the beaker and diluting it by a factor of 10. The colloidal suspensions were adjusted to the appropriate pH (typically 8.75) using 0.01 M HCl .

$\text{Si}(100)$ substrates (1 cm^2) were cleaned by sonicating for 15 min in piranha solution (1:4 30% H_2O_2 :98% H_2SO_4), which formed a 15–20 Å SiO_2 layer. The substrates were washed

(11) Mallouk, T. E.; Kim, H.-N.; Ollivier, P. J.; Keller, S. W. In *Comprehensive Supramolecular Chemistry*; Alberti, G., Bein, T., Eds.; Elsevier Science: Oxford, UK, 1996; Vol. 7, pp 189–218.

(12) Treacy, M. M. J.; Rice, S. B.; Jacobson, A. J.; Lewandowski, J. T. *Chem. Mater.* **1990**, *2*, 279.

(13) Fang, M.; Kim, H. N.; Saupé, G. B.; Miwa, T.; Fujishima, A.; Mallouk, T. E. *Chem. Mater.* **1999**, *11*, 1526.

(14) Schaak, R. E.; Mallouk, T. E. *Chem. Mater.* **2000**, *12*, 2513.

(15) (a) Dion, M.; Ganne, M.; Tournoux, M. *Mater. Res. Bull.* **1981**, *16*, 1429. (b) Jacobson, A. J.; Johnson, J. W.; Lewandowski, J. T. *Inorg. Chem.* **1985**, *24*, 3727.

(16) Uma, S.; Gopalakrishnan, J. *Chem. Mater.* **1994**, *6*, 907.

(17) Gopalakrishnan, J.; Uma, S.; Bhat, V. *Chem. Mater.* **1993**, *5*, 132.

(18) Uma, S.; Raju, A. R.; Gopalakrishnan, J. *J. Mater. Chem.* **1993**, *3*, 709.

(19) Ram, R. A. M.; Clearfield, A. *J. Solid State Chem.* **1994**, *112*, 288.

(20) Ruddlesden, S. N.; Popper, P. *Acta Crystallogr.* **1957**, *10*, 538; *Acta Crystallogr.* **1958**, *11*, 54.

(21) Thangadurai, V.; Subbanna, G. N.; Gopalakrishnan, J. *Chem. Commun.* **1998**, 1300.

(22) Ollivier, P. J.; Mallouk, T. E. *Chem. Mater.* **1998**, *10*, 2585.

(23) Geselbracht, M. J.; Macdonald, L. S.; Scarola, R. J. *Book of Abstracts*; 213th ACS National Meeting, San Francisco, April 13–17 1997, INOR-118.

(24) Schaak, R. E.; Mallouk, T. E., *J. Solid State Chem.* In press.

(25) Gopalakrishnan, J.; Bhat, V. *Inorg. Chem.* **1987**, *26*, 4301.

(26) (a) Bhuvanesh, N. S. P.; Crosnier-Lopez, M. P.; Duroy, H.; Fourquet, J. L. *J. Mater. Chem.* **1999**, *9*, 3093. (b) Yoon, S. H.; Yoon, J. J.; Lee, S. O. *J. Solid State Chem.* **1996**, *127*, 119.

with copious amounts of water, dried with Ar, and then placed in 20 mM poly(diallyldimethylammonium chloride) (PDDA) at room temperature. After 5 min, the substrates were removed from the PDDA solution, washed, and dried. The derivatized substrates were then placed in the diluted, pH-adjusted colloidal suspension at 30 °C for 20 min in a procedure described in detail elsewhere.¹⁴ The substrate was then removed, washed with water, and dried with Ar.

For some of the systems, poly(allylamine hydrochloride) (PAH) was used instead of PDDA. In these cases, the Si(100) surface was cleaned in piranha and then washed and dried before being placed in a 2% solution of (4-aminobutyl)-dimethylmethoxysilane (4-ABDMMS) in dry toluene for 15 h in a desiccator. The substrates were then removed from the 4-ABDMMS solution, washed with toluene, toluene/methanol, and methanol, and then dried with Ar. The derivatized substrates were immediately placed in 20 mM poly(sodium styrenesulfonate) (PSS) for 15 min and then washed and placed in 20 mM PAH for 15 min, and the process was repeated. After two PSS/PAH bilayers were formed, the samples were washed with water, dried with Ar, and then placed in the diluted, pH-adjusted colloidal suspension for 30 min at room temperature. After 30 min, the samples were removed, washed with water, and dried with Ar.

Instrumentation. Powder X-ray diffraction (XRD) patterns were obtained on a Philips X-Pert MPD diffractometer using monochromatized Cu K α ($\lambda = 1.5418 \text{ \AA}$) radiation. Diffraction patterns from powdered samples held on a quartz zero background plate were obtained in θ – θ geometry.

TEM images were obtained using a JEOL 1200EXII microscope at 80 kV at the Electron Microscope Facility for the Life Sciences at the Biotechnology Institute at the Pennsylvania State University. (The monodisperse scrolls formed from the exfoliation of H₂La₂Ti₃O₁₀ were imaged at 120 kV.) The colloids were imaged on Formvar-coated Cu grids.

Atomic force microscope (AFM) images were obtained using a Nanoscope IIIA AFM in tapping mode.

Elemental analysis for C, H, and N were performed by Atlantic Microlabs, Inc., Norcross, GA.

Results and Discussion

Interlayer Acidity of Protonated Ruddlesden–Popper Phases. One of the necessary prerequisites for exfoliation is the ability of the protonated layered perovskite to intercalate organic bases. Gopalakrishnan and co-workers found that for the Dion–Jacobson phases that span the HCa_{2–x}La_xNb_{3–x}Ti_xO₁₀ series,¹⁷ stoichiometric intercalation of *n*-alkylamines occurs for the $x = 0, 1$ members (HCa₂Nb₃O₁₀ and HCaLaNb₂TiO₁₀). In contrast, the $x = 2$ member (HLa₂Ti₂NbO₁₀) only partially intercalated stronger organic bases such as piperidine. The weaker acidity in HLa₂Ti₂NbO₁₀ was attributed to the intrinsic acidity of the M–O bonds, since Ti–O–H is less acidic than Nb–O–H. In a parallel study of the layered perovskites H_{2–x}La₂Ti_{3–x}Nb_xO₁₀, which bridge the Dion–Jacobson and Ruddlesden–Popper series, the $x = 2$ Ruddlesden–Popper end member H₂La₂Ti₃O₁₀ did not intercalate any organic bases, even after extended periods of time.¹⁸ The reason was attributed to the coordination of the protons nested in the semi-cubooctahedral cavities between the staggered layers, which are structurally inaccessible to intercalation. This idea was supported by studying H₂Ca₂Nb₂TiO₁₀, which has the same staggered interlayer environment, but more acidic Nb–O–H protons. As expected, H₂Ca₂Nb₂TiO₁₀ did not intercalate organic bases.¹⁸

While the interlayer galleries of the Ruddlesden–Popper phases appear inaccessible to intercalation, the

recent results of Geselbracht and co-workers with Ta-containing Dion–Jacobson phases²³ suggest another approach. The protons on the (Ti,Nb)O₆ octahedra are weakly acidic, so there is not much of a driving force for neutralization with a base. However, if the Ti⁴⁺ and Nb⁵⁺ atoms were replaced by Ta⁵⁺, which appears more acidic than Nb⁵⁺ in the layered perovskites, then it may be possible to induce intercalation of a strong organic base, despite the structural features of the lamellar phase. While the oxides of Ta⁵⁺ might be expected to be less acidic than Nb⁵⁺ oxides on the basis of periodic electronegativity trends, the subtle structural differences between the niobate and tantalate perovskites is apparently sufficient to cause the reverse trend in acidity. The MO₆ octahedra in the niobates are more distorted than in the tantalates, leading to a shorter terminal M–O bond in the niobates. This means that the nonterminal, bridging oxygen atoms that closely coordinate H in the Ruddlesden–Popper phases are more negatively charged, and therefore more basic, in the niobates than in the tantalates.

Fortunately, stoichiometric intercalation of an organic base is not necessary for exfoliation, since delamination occurs when only a fraction of the interlayer protons are neutralized by a strong, bulky organic base. For example, HCa₂Nb₃O₁₀ exfoliates when only 15–20% of the protons are replaced with bulky TBA⁺ groups.¹⁴ In other cases, 30–50% intercalation is ideal for delamination to occur.¹³ Therefore, the Dion–Jacobson phase HLa₂Ti₂NbO₁₀, which does not intercalate *n*-alkylamines and only intercalates a substoichiometric amount of piperidine,^{17,18} exfoliates upon partial intercalation of TBA⁺. Likewise, Ruddlesden–Popper phases that are specifically tailored to have more acidic interlayer protons by placing Ta⁵⁺ in the MO₆ octahedra should also intercalate at least a small amount of a strong organic base, which should be sufficient for delamination to occur.

Preliminary evidence suggests that the protonated Ruddlesden–Popper tantalates intercalate *n*-alkylamines, which typically have p*K*_b values near 3.4 (compared to piperidine, which has p*K*_b = 2.70). For example, H₂CaNaTa₃O₁₀, which is isostructural with H₂La₂Ti₃O₁₀, was found by XRD to intercalate *n*-decylamine (p*K*_b = 3.36) upon reaction in hexane at 60 °C for several days. (For consistency and comparison with previously reported results, the intercalated phases were annealed at 100 °C for several hours prior to XRD analysis, according to the method of Gopalakrishnan and co-workers.^{17,18}) The presence of a low-angle reflection at 3.51° 2 θ ($d = 25.12 \text{ \AA}$) in the diffraction pattern of (C₁₀H₂₁NH₃)_xH_{2–x}CaNaTa₃O₁₀, shown in Figure 1a, indicates that the interlayer gallery is expanded by 11.63 Å relative to H₂CaNaTa₃O₁₀, which has a low-angle peak at 6.55° 2 θ ($d = 13.49 \text{ \AA}$).¹⁹ While a series of (00*l*) peaks is evident in the pattern, it is clear that intercalation is not complete. The unindexed peaks in Figure 1a correspond to the parent compound H₂CaNaTa₃O₁₀ (Figure 1b) as well as the defect perovskite phase CaNaTa₃O₉, which forms from the low-temperature topochemical dehydration of H₂CaNaTa₃O₁₀.¹⁹ The incomplete intercalation reaction could in this case represent an equilibrium product distribution, as in

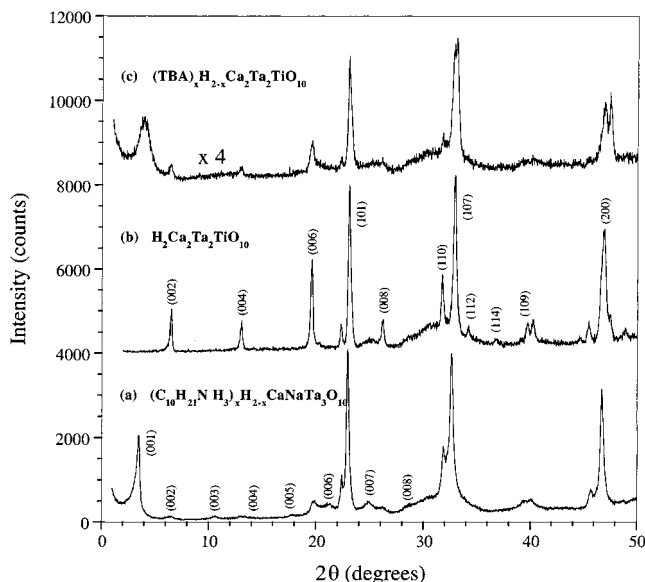


Figure 1. XRD patterns of (a) $(\text{C}_{10}\text{H}_{21}\text{NH}_3)_x\text{H}_{2-x}\text{CaNaTa}_3\text{O}_{10}$, (b) $\text{H}_2\text{Ca}_2\text{Ta}_2\text{TiO}_{10}$, and (c) $\text{TBA}_x\text{H}_{2-x}\text{Ca}_2\text{Ta}_2\text{TiO}_{10}$. The vertical scale in part c is expanded by a factor of 4.

$\text{HLa}_2\text{Ti}_2\text{NbO}_{10}$, or it could be due to kinetic factors or unoptimized reaction conditions.

Exfoliation of Ruddlesden–Popper Phases. As expected from their reactivity with alkylamines, all of the tantalate and titanotantalate phases readily exfoliate when exposed to TBA^+OH^- , and some of the titanates and titanoniobates also exfoliate at least partially. In no case is the reaction 100% complete, presumably due to kinetic factors, unexchanged alkali cations, or regions otherwise inaccessible to intercalation. This occurs even in the easily exfoliated Dion–Jacobson series and is typically not problematic when using the colloids as building blocks for thin films. The unexfoliated material is usually more dense and can often be separated, since it quickly settles to the bottom of the colloidal suspension. Many Ruddlesden–Popper phases cannot be synthesized without perovskite or other impurities (e.g. $\text{H}_2\text{Sr}_2\text{Ta}_2\text{TiO}_{10}$).¹⁹ However, by making unilamellar colloids from the Ruddlesden–Popper phases and allowing the unreactive impurities to settle to the bottom, it is possible to utilize even the impure phases as colloidal building blocks.

The most acidic $n = 3$ phase, $\text{H}_2\text{CaNaTa}_3\text{O}_{10}$, delaminates relatively well. Reacting $\text{H}_2\text{CaNaTa}_3\text{O}_{10}$ with a 30-fold excess of TBA^+OH^- for 1 week at room temperature produces the exfoliated colloid $\text{TBA}_x\text{H}_{2-x}\text{CaNaTa}_3\text{O}_{10}$. A TEM image of this colloid is shown in Figure 2a. Interestingly, some of the colloidal particles remain as sheets, while others curl to form nanoscale scrolls. The $\text{TBA}_x\text{H}_{2-x}\text{CaNaTa}_3\text{O}_{10}$ sheets have lateral dimensions of around 100–400 nm, and the lengths of the scrolls are similar. As in images of colloids made from Dion–Jacobson phases,¹⁴ the presence of many sheets of identical contrast is consistent with the idea of exfoliation to unilamellar (in this case, three octahedra thick) colloidal particles.

The $n = 3$ titanotantalates $\text{H}_2\text{A}_2\text{Ta}_2\text{TiO}_{10}$ and $\text{H}_2\text{ALaTi}_2\text{TaO}_{10}$ ($A = \text{Ca}, \text{Sr}$) also exfoliate upon reaction with TBA^+OH^- . While the all-tantalum phase tends to form sheets and scrolls, the titanotantalates form only sheets. Sheets of $\text{TBA}_x\text{H}_{2-x}\text{SrLaTi}_2\text{TaO}_{10}$, shown in

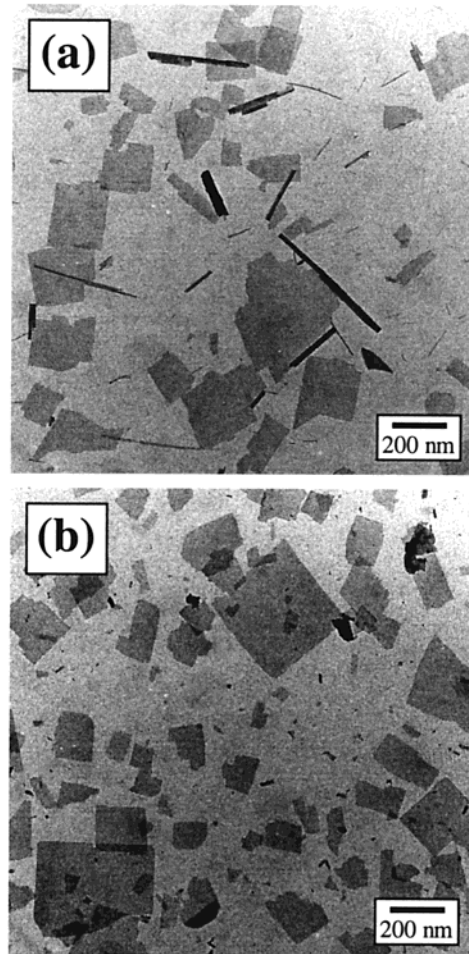


Figure 2. TEM micrographs of (a) colloidal sheets and scrolls of $\text{TBA}_x\text{H}_{2-x}\text{CaNaTa}_3\text{O}_{10}$ and (b) sheets of $\text{TBA}_x\text{H}_{2-x}\text{SrLaTi}_2\text{TaO}_{10}$.

Figure 2b, are largely rectangular and are approximately the same size as those of $\text{TBA}_x\text{H}_{2-x}\text{CaNaTa}_3\text{O}_{10}$. The $\text{TBA}_x\text{H}_{2-x}\text{CaLaTi}_2\text{TaO}_{10}$ and $\text{TBA}_x\text{H}_{2-x}\text{A}_2\text{Ti}_2\text{TaO}_{10}$ sheets look similar. The XRD pattern (Figure 1c) of $\text{TBA}_x\text{H}_{2-x}\text{Ca}_2\text{Ta}_2\text{TiO}_{10}$, collected by centrifuging the suspended colloid, shows a low-angle reflection at 4.11° 2θ ($d = 21.50 \text{ \AA}$). This low-angle peak is consistent with the XRD patterns of other exfoliated phases that restack, yielding broad $(00l)$ reflections and no (hkl) peaks, since a- and b-axis registry is lost upon exfoliation. The sharper, higher angle ($>6^\circ$ 2θ) peaks in Figure 1c match those of $\text{H}_2\text{Ca}_2\text{Ta}_2\text{TiO}_{10}$, which provides evidence that the exfoliation was not complete. However, the $\text{H}_2\text{Ca}_2\text{Ta}_2\text{TiO}_{10}$ peaks are broader than in the unreacted solid, which suggests that this phase comes from a fraction of the sample that was intercalated or partially intercalated, but never exfoliated. Note that the intensity of the diffraction peaks in Figure 1c is quite low relative to the alkylamine intercalation compound (Figure 1a) or the parent compound $\text{H}_2\text{Ca}_2\text{Ta}_2\text{TiO}_{10}$ (Figure 1b). This implies that most of the restacked material is in fact amorphous to X-rays.

The $n = 2$ tantalate, $\text{H}_2\text{SrTa}_2\text{O}_7$, also delaminates upon reaction with TBA^+OH^- . Interestingly, exfoliated $\text{TBA}_x\text{H}_{2-x}\text{SrTa}_2\text{O}_7$ predominantly forms scrolls that span a wide range of sizes. Figure 3a shows a group of $\text{TBA}_x\text{H}_{2-x}\text{SrTa}_2\text{O}_7$ scrolls that range in length from several hundred nanometers to $6 \mu\text{m}$ or larger. In

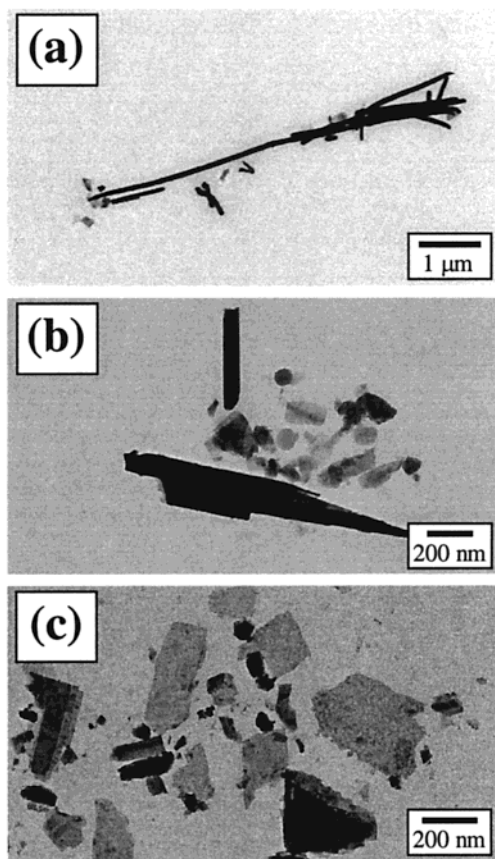


Figure 3. TEM micrographs of (a) large scrolls of $\text{TBA}_x\text{H}_{2-x}\text{SrTa}_2\text{O}_7$, (b) smaller scrolls and sheets of $\text{TBA}_x\text{H}_{2-x}\text{SrTa}_2\text{O}_7$, and (c) sheets of $\text{TBA}_x\text{H}_{2-x}\text{SrNb}_2\text{O}_7$, in addition to some unexfoliated material.

contrast, Figure 3b shows a bundle of $\text{TBA}_x\text{H}_{2-x}\text{SrTa}_2\text{O}_7$ scrolls that are less than $1\ \mu\text{m}$ in length, as well as several sheets that have lateral dimensions of $50\text{--}200\ \text{nm}$. While the sheets and scrolls of the colloid $\text{TBA}_x\text{H}_{2-x}\text{CaNaTa}_3\text{O}_{10}$ are approximately the same size, the $\text{TBA}_x\text{H}_{2-x}\text{SrTa}_2\text{O}_7$ scrolls are 1–2 orders of magnitude longer than the largest dimensions of the sheets. Apparently, if the exfoliation reaction produces large ($>200\ \text{nm}$) sheets, the sheets prefer to curl into scrolls, while smaller sheets are stable without curling. Bundles of scrolls aligned end-to-end and side-to-side were frequently observed in the $\text{TBA}_x\text{H}_{2-x}\text{SrTa}_2\text{O}_7$ system, which can give the appearance of longer or thicker tubes. Detailed high-resolution electron microscopy and cross-sectional analysis of the scrolls are in progress to fully understand the formation and structure of the largest scrolls, as well as to confirm that they are hollow scrolls rather than bulk-phase needlelike crystals.

While all of the tantalates and titanotantalates readily exfoliate, the Ruddlesden–Popper titanates and titanoniobates either do not exfoliate at all or exfoliate only to a limited extent. The $n = 2$ niobate $\text{H}_2\text{SrNb}_2\text{O}_7$ exfoliates only minimally and only after a long reaction time (several weeks). In contrast to the $n = 2$ tantalate, $\text{TBA}_x\text{H}_{2-x}\text{SrNb}_2\text{O}_7$ forms sheets instead of tubes. The TEM micrograph of the $\text{TBA}_x\text{H}_{2-x}\text{SrNb}_2\text{O}_7$ sheets in Figure 3c shows $100\text{--}400\ \text{nm}$ sheets, as well as a significant amount of unexfoliated material, which is typical for all of the titanates and titanoniobates. The $n = 3$ phase $\text{H}_2\text{Ca}_2\text{Nb}_2\text{TiO}_{10}$, the titanoniobate analogue of $\text{H}_2\text{Ca}_2\text{Ta}_2\text{TiO}_{10}$, also exfoliates to a limited extent and,

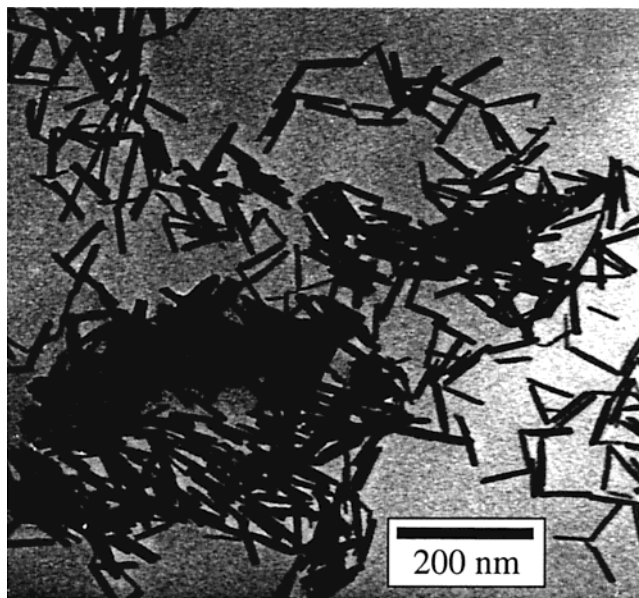


Figure 4. TEM micrograph of monodisperse nanoscale scrolls formed from the exfoliation of $\text{H}_2\text{La}_2\text{Ti}_3\text{O}_{10}$ using a polymeric amine.

unlike $\text{TBA}_x\text{H}_{2-x}\text{Ca}_2\text{Ta}_2\text{TiO}_{10}$, the $\text{TBA}_x\text{H}_{2-x}\text{Ca}_2\text{Nb}_2\text{TiO}_{10}$ colloids form a mixture of sheets and scrolls.

A careful study of the exfoliation behavior of the $\text{H}_2\text{La}_2\text{Ti}_3\text{O}_{10}$ system yielded some surprising results. While X-ray diffraction and C, H, N analysis provided little evidence for the intercalation of TBA^+ into the bulk solid, a microscopic study of the supernatant solution revealed that some intercalation must have occurred. The intercalation reaction occurs inward from the edges of the crystallites, so the interlayer gallery may be sufficiently inaccessible (combined with the weak acidity of the $\text{Ti}\text{--}\text{O}\text{--}\text{H}$ protons) that exfoliation occurs only over extremely long reaction times (weeks to months). In the following examples, the exfoliation reaction was typically allowed to occur for 2–4 weeks. Even after such a long reaction time, only a small percentage of the bulk solid intercalated the organic bases.

Reacting $\text{H}_2\text{La}_2\text{Ti}_3\text{O}_{10}$ with a 30-fold molar excess of TBA^+OH^- produces, at times, a few sheets and scrolls that vary in size. In no case are $\text{TBA}_x\text{H}_{2-x}\text{La}_2\text{Ti}_3\text{O}_{10}$ colloids observed without a significant amount of unexfoliated material. However, upon reaction of an aqueous solution of *n*-butylamine with $\text{H}_2\text{La}_2\text{Ti}_3\text{O}_{10}$, sheets were produced. Interestingly, these sheets are about $500\ \text{nm}$ to $1\ \mu\text{m}$ in length, which is larger than those of most other $n = 3$ phases. In an attempt to prop open the interlayer gallery and avoid the less-reactive $\text{H}_2\text{La}_2\text{Ti}_3\text{O}_{10}$ intermediate, the alkali parent $\text{K}_2\text{La}_2\text{Ti}_3\text{O}_{10}$ was reacted with a saturated NaCl solution for 1 week. The resulting $\text{Na}_2\text{La}_2\text{Ti}_3\text{O}_{10}\cdot x\text{H}_2\text{O}$ phase was reacted with TBA^+OH^- , and large sheets were also formed.

We also attempted to exfoliate $\text{H}_2\text{La}_2\text{Ti}_3\text{O}_{10}$ using *O*-(2-aminopropyl)-*O'*-(2-methoxyethyl) polypropylene glycol 500, which is one of the polymeric amines originally used by Treacy et al. to exfoliate $\text{HCa}_2\text{Nb}_3\text{O}_{10}$.¹⁰ Surprisingly, scrolls that are ca. $20 \times 100\ \text{nm}$ were formed almost exclusively. These scrolls, shown in Figure 4, are very monodisperse. A few $100 \times 400\ \text{nm}$ sheets were occasionally found among the scrolls, which provides good evidence that the tubes form from nearly

monodisperse sheets. It is unclear why the polymeric surfactant causes the scrolls to be monodisperse. It is possible that the surfactant chain acts as a template for the sheets to curl around, and the sheets naturally cleave when rolls or sheets of a particular size have formed.

While the $n = 3$ titanate $\text{H}_2\text{La}_2\text{Ti}_3\text{O}_{10}$ exhibits interesting, although limited, exfoliation behavior, the $n = 1$ phase HLaTiO_4 does not exfoliate under any conditions. Raman spectra of HLaTiO_4 indicate that the protons are not very acidic,²⁷ just as in $\text{H}_2\text{La}_2\text{Ti}_3\text{O}_{10}$. However, the marked difference in exfoliation behavior between the two may lie in their ionic character. HLaTiO_4 , which has a rocksalt-type layer of La^{3+} only a single perovskite block away from the protonated interlayer gallery, is held together more strongly by ionic interactions than $\text{H}_2\text{La}_2\text{Ti}_3\text{O}_{10}$, in which the triple perovskite block is more covalent.

Sheet vs Scroll Formation in the Exfoliated Perovskites. The most puzzling aspect of the exfoliation behavior of the Ruddlesden–Popper phases is their unpredictable tendency to curl and form scrolls rather than sheets, and there are several possible explanations for why they do so. In some systems such as halloysite²⁸ and $\text{H}_{3.2}\text{K}_{0.8}\text{Nb}_6\text{O}_{17}$,²⁹ exfoliated sheets curl to relieve built-in strain due to their noncentrosymmetric structure. However, crystallographic studies of all of the bulk perovskite phases indicate that they are centrosymmetric. In addition, careful analysis of the XRD data (including Rietveld structure refinement) indicates that the parent layered materials are phase pure. In some cases (e.g. $\text{H}_2\text{SrLaTi}_2\text{TaO}_{10}$), an ABO_3 perovskite impurity is present,²⁴ but is unreactive during the low-temperature intercalation reactions. Thus, all of the exfoliated colloids (sheets, scrolls, or both) appear to be derived from single-phase materials.

One explanation for the formation of scrolls is that, upon exfoliation, the individual sheets have asymmetric distributions of A- or B-site cations, creating a polarization that is relieved by curling. This could account for the curling of $\text{TBA}_x\text{H}_{2-x}\text{CaNaTa}_3\text{O}_{10}$ colloids, for example, in which Ca and Na could preferentially fill the A sites in alternate layers. (EDAX analysis does not show a statistically significant difference between the elemental composition of the sheets and scrolls.) However, this would not explain the tendency of colloids derived from $\text{H}_2\text{SrTa}_2\text{O}_7$ or $\text{H}_2\text{La}_2\text{Ti}_3\text{O}_{10}$ to curl. A second possibility is that the sheets curl as a result of cooperative distortions of the MO_6 octahedra, which is frequently observed in displacive ferroic phase transitions in perovskites.³⁰

Another possibility is that the curling may be due to the intrinsic bonding character of water or the intercalated base with the interlayer atoms of the perovskite block. It has been found in many Ruddlesden–Popper systems, including $\text{NaEuTiO}_4 \cdot 0.8\text{H}_2\text{O}$,³¹ $\text{K}_2\text{SrTa}_2\text{O}_7 \cdot$

$2\text{H}_2\text{O}$,³² and $\text{K}_2\text{Ca}_2\text{Ta}_2\text{TiO}_{10} \cdot 0.8\text{H}_2\text{O}$,²⁴ that intercalated water in the hydrated phases causes a significant distortion of the MO_6 octahedra. Likewise, a detailed Raman study of layered perovskites concluded that the nature of the interlayer A' cation has a major impact on the bonding characteristics and distortions of the MO_6 octahedra.³³ Clearly, any changes in the interlayer coordination and bonding will affect the bonding in the MO_6 octahedra.

It is possible that, upon intercalation, the quaternary ammonium species and the polymeric amine cause localized distortions in some of the single-crystal colloids, which create local polar regions in the crystal that induce curling. In the case of $\text{H}_2\text{La}_2\text{Ti}_3\text{O}_{10}$, the interlayer bonding with the n -alkylamine may not significantly alter the MO_6 octahedra. The curling may, therefore, be correlated to the amount (and/or location) of the organic base intercalated into the interlayer. Stoichiometric intercalation (which is possible for aliphatic amines but not for the bulky quaternary amines) would displace the octahedra equally at every site, so the symmetry would remain centrosymmetric and no curling would occur. Unfortunately, since many of these systems have impurities and only a small percentage of the solid exfoliates, quantitation of the amount of intercalated base is difficult. In the $\text{Na}_2\text{La}_2\text{Ti}_3\text{O}_{10} \cdot x\text{H}_2\text{O}$ system, not all of the Na^+ will be displaced by TBA^+ , and the remaining Na^+ may be enough to maintain the centrosymmetric interlayer bonding of the alkali precursor.

Regardless, there is still not a clear understanding of how intercalation affects the interlayer bonding and why certain Ruddlesden–Popper phases (as well as some Dion–Jacobson phases) curl rather than remain as sheets. Detailed crystallographic and Raman/IR studies of amine-intercalated solids may help us to understand the interlayer bonding and distortions. Unfortunately, since most of the intercalated phases are less crystalline than their precursors, X-ray structural studies often prove difficult.

Assembly of Perovskite Monolayers. Like the exfoliated Dion–Jacobson phases, the new Ruddlesden–Popper colloids can be electrostatically adsorbed to a surface that has been derivatized with a polycation. Figure 5a shows an AFM image of $\text{TBA}_x\text{H}_{2-x}\text{CaNaTa}_3\text{O}_{10}$ sheets and scrolls on a Si/SiO_2 surface that has been derivatized with poly(diallyldimethylammonium chloride) (PDDA). Sheets of $\text{TBA}_x\text{H}_{2-x}\text{Ca}_2\text{Ta}_2\text{TiO}_{10}$ adsorbed to the $\text{Si}/\text{SiO}_2/\text{PDDA}$ surface are shown in Figure 5b. In all cases, the sheets and scrolls tend to form a monolayer, although there is some overlap of sheets. Also, the sheets do not self-assemble into tiled monolayers like many of the Dion–Jacobson phases.¹⁴ Presumably, the Ruddlesden–Popper sheets have a higher surface charge than the Dion–Jacobson colloids and, therefore, irreversibly stick to the cationic surface. Only a small amount of overlap between the anionic sheets and the highly charged cationic polymer is necessary for the sheets to stick irreversibly, despite the anion–anion repulsion of the overlapping sheets.

While PDDA has a high positive charge density at all pH values, the surface charge of PAH is strongly

(27) Byeon, S. H.; Lee, S. O.; Kim, H. J. *Solid State Chem.* **1997**, *130*, 110.

(28) Frazier, S. E.; Bedford, J. A.; Hower, J.; Kenney, M. E. *Inorg. Chem.* **1968**, *6*, 1693.

(29) Saupe, G. B.; Waraksa, C. C.; Kim, H. N.; Han, Y. J.; Kaschak, D. M.; Skinner, D. M.; Mallouk, T. E. *Chem. Mater.* **2000**, *12*, 1556.

(30) Lines, M. E.; Glass, A. M. *Principles and Applications of Ferroelectrics and Related Materials*; Clarendon Press: Oxford, 1977.

(31) Toda, K.; Kameo, Y.; Kurita, S.; Sato, M. *Bull. Chem. Soc. Jpn.* **1996**, *69*, 349.

(32) Kodenkandath, T. A.; Wiley, J. B. *Mater. Res. Bull.* In press.

(33) Byeon, S. H.; Nam, H. J. *Chem. Mater.* **2000**, *12*, 1771.

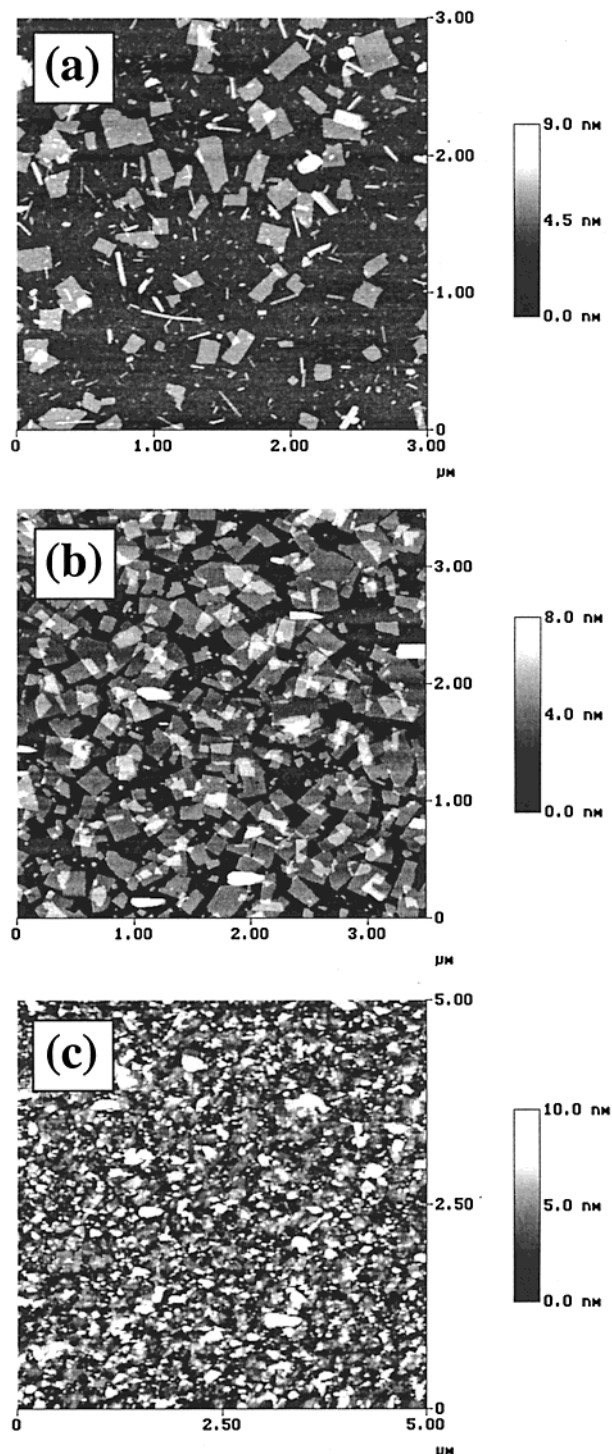


Figure 5. AFM images of (a) $\text{TBA}_x\text{H}_{2-x}\text{CaNaTa}_3\text{O}_{10}$ and (b) $\text{TBA}_x\text{H}_{2-x}\text{Ca}_2\text{Ta}_2\text{TiO}_{10}$ on $\text{Si/SiO}_2/\text{PDDA}$. $\text{TBA}_x\text{H}_{2-x}\text{SrLaTi}_2\text{TaO}_{10}$ sheets on $\text{Si/SiO}_2/4\text{-ABDMMS}/(\text{PSS}/\text{PAH})_2$ are shown in part c.

dependent on pH. In some systems, such as HTiNbO_5^9 and $\alpha\text{-Zr}(\text{HPO}_4)_2\cdot\text{H}_2\text{O}$,⁸ careful control over the pH allows self-assembled tiled monolayers to form. In these cases, intermediate pH values provide the sheets and polycation with moderate charge that allows the sheets to adhere reversibly to the surface so that they can move around to adopt the most stable conformation, which is when the sheets cover the entire surface without overlapping.

A pH study of the $\text{TBA}_x\text{H}_{2-x}\text{SrLaTi}_2\text{TaO}_{10}$ system showed that at low pH (8–8.7), surface coverage on PAH

was moderate, as expected. At moderate pH values (8.8–9.4), coverage tended to be higher, but submonolayer coverage was still observed. At a high pH (above 9.5), the sheets assembled into tiled monolayers, as shown in Figure 5c. At such a high pH, the positive charge on the PAH surface is minimal, while the sheets are highly anionic. The low charge on the polycation apparently favors the lateral mobility of the sheets, which can move around to completely cover the surface. Unfortunately, the $\text{TBA}_x\text{H}_{2-x}\text{SrLaTi}_2\text{TaO}_{10}$ sample contains a large amount of either unexfoliated or hydrolyzed material, which is evident by the irregular features in Figure 5c that appear higher than the sheets. (Similar features are evident as irregularly shaped black spots in the TEM micrograph in Figure 2b.)

An interesting feature of the nontantalate Ruddlesden–Popper colloids is that, although they can minimally exfoliate, they do not readily stick to a cationic surface. For example, while the $\text{TBA}_x\text{H}_{2-x}\text{SrTa}_2\text{O}_7$ scrolls stick reasonably well to a $\text{Si/SiO}_2/\text{PDDA}$ surface, the $\text{TBA}_x\text{H}_{2-x}\text{SrNb}_2\text{O}_7$ sheets do not. Likewise, while $\text{TBA}_x\text{H}_{2-x}\text{Ca}_2\text{Ta}_2\text{TiO}_{10}$ sheets cover the PDDA-derivatized surface, the niobate $\text{TBA}_x\text{H}_{2-x}\text{Ca}_2\text{Nb}_2\text{TiO}_{10}$ sticks only minimally.

In order for the sheets to stick to the cationic surface, protonated amine groups of the surface-bound polymer must displace the loosely bound TBA^+ cations on the colloidal sheets. For weakly acidic systems such as the Ruddlesden–Popper titanates and titanoniobates, the exfoliated colloids may have insufficient negative charge at the pH where the surface polycation is protonated (in the case of PAH) or to bind to well to “soft” polycations such as PDDA. Some support for this idea comes from a study of the exfoliated Dion–Jacobson phase $\text{HLa}_2\text{Ti}_2\text{NbO}_{10}$, which was found by Gopalakrishnan and co-workers to intercalate only a small amount of organic base, indicating that it is only weakly acidic.^{17,18} We found that this compound exfoliates in TBA^+OH^- almost as readily as $\text{HCa}_2\text{Nb}_3\text{O}_{10}$, but its surface coverage on PDDA or PAH is minimal. The weakly acidic Ti^{4+} cations, which are likely concentrated along the interlayer gallery of the bulk solid¹⁷ and, therefore, are on the outer face of the colloid, do not allow sufficient ionization for strong electrostatic binding to the surface.

As expected, the exfoliated derivatives of $\text{H}_2\text{La}_2\text{Ti}_3\text{O}_{10}$ generally do not adhere to any positively charged surface. (The monodisperse scrolls minimally adsorb to a PDDA surface.) For the titanate exfoliated using *n*-butylamine, it is likely that the amine is held more tightly to the surface of the colloid than the larger TBA^+ cations, so displacement in favor of the amine on the polymer is highly disfavored. Likewise, the exfoliated $\text{Na}_2\text{La}_2\text{Ti}_3\text{O}_{10}\cdot x\text{H}_2\text{O}$, which contains terminal Na^+ cations on the surface of the colloid, does not stick to a PDDA or PAH surface, because the small Na^+ cation is not displaced in favor of the larger amine. This is also the case for the colloidal scrolls of the Dion–Jacobson phase $\text{NaPb}_2\text{Nb}_3\text{O}_{10}$, which was exfoliated using *n*-propylamine.¹³ These scrolls also do not adhere to polycationic surfaces.

Conclusions

Compositionally tailored Ruddlesden–Popper phases that have acidic interlayer protons attached to TaO_6 or

(Ta,Ti)O₆ octahedra have been shown to exfoliate into colloidal sheets and nanoscale scrolls. While protonated Ruddlesden–Popper phases were thought to be structurally inaccessible to intercalation by organic bases, it appears that the interlayer structural features primarily affect the kinetics of the intercalation reaction. Neutralization of the acidic Ta–O–H protons by a strong organic base is a sufficient driving force to overcome the structural barrier to intercalation. Exfoliation is minimal for other titanate and titanoniobate Ruddlesden–Popper phases, and their ability to adsorb to a surface-bound polycation is highly dependent on their acidity. However, some of the resulting colloids, such as the monodisperse scrolls formed by exfoliation of H₂La₂Ti₃O₁₀, could be interesting building blocks for nanoscale assemblies.

The present study opens up some interesting areas for future research. Recently, Sugahara et al. reported a reaction that converts Aurivillius phases, which are perovskite–bismuth oxide intergrowths, into protonated Ruddlesden–Popper phases by selectively leaching the Bi₂O₂ sheets with acid.³⁴ This reaction could provide a variety of new protonated Ruddlesden–Popper phases that may be amenable to exfoliation. For example, the phase with the nominal composition H₂SrNaNb₃O₁₀, obtained from Bi₂O₂[SrNaNb₃O₁₀], was found to intercalate *n*-alkylamines³⁴ (similarly to H₂CaNaTa₃O₁₀ in this report), so it should also react with stronger bases such as TBA⁺OH⁻. Also, the reduced tantalate Na₂Ca₂Ta₃O₁₀ (obtained by reductive intercalation of the Dion–Jacobson phase NaCa₂Ta₃O₁₀)³⁵ and the reduced niobate Rb₂LaNb₂O₇ (obtained by reductive intercalation of

RbLaNb₂O₇)³⁶ have mixed-valent Ta^{4+/5+} and Nb^{4+/5+}, respectively. Attempts at ion-exchange and exfoliation of these reduced phases may prove interesting, since their acidities should be intermediate between the M⁵⁺ and Ti⁴⁺ phases.

It is now possible to view the wide range of Ruddlesden–Popper phases that have been synthesized both directly and topochemically as potential building blocks to new nanostructured materials. Combined with the exfoliated Dion–Jacobson phases, a wide range of stoichiometries and stacking sequences should be accessible in thin film heterostructures. It may also be possible to apply to the thin films the topochemical reactions that convert lamellar phases into A-site defective^{21,22,25,37} and nondefective³⁸ three-dimensional perovskites. Additionally, incorporating reducible cations such as Cu^{2+/3+}, Mn⁴⁺, or Ru⁴⁺ (which has recently been reported by Wiley et al.³⁹) into the B-sites of layered perovskites could provide new routes to thin films that possess interesting electronic properties.

Acknowledgment. This work was supported by National Science Foundation grant CHE-9529202. Instrumentation for AFM experiments was provided by National Science Foundation grant CHE-9626326. This material is based upon work supported under a National Science Foundation Graduate Fellowship.

CM000495R

(34) Sugimoto, W.; Shirata, M.; Sugahara, Y.; Kuroda, K. *J. Am. Chem. Soc.* **1999**, *121*, 11601.

(35) Toda, K.; Takahashi, M.; Teranishi, T.; Ye, Z. G.; Sato, M.; Hinatsu, Y. *J. Mater. Chem.* **1999**, *9*, 799.

(36) Armstrong, A. R.; Anderson, P. A. *Inorg. Chem.* **1994**, *33*, 4366.

(37) Fang, M.; Kim, C. H.; Mallouk, T. E. *Chem. Mater.* **1999**, *11*, 1519.

(38) Schaak, R. E.; Mallouk, T. E. *J. Am. Chem. Soc.* **2000**, *122*, 2798.

(39) Lalena, J. N.; Falster, A. U.; Simmons, W. B.; Carpenter, E. E.; Wiggins, J.; Hariharan, S.; Wiley, J. B. *Chem. Mater.* **2000**, *12*, 2418.